



## LJMU Research Online

Wang, X, O'Reilly, AO, Williamson, MS, Puinean, AM, Yang, Y, Wu, S and Wu, Y

**Function and pharmacology of glutamate-gated chloride channel exon 9 splice variants from the diamondback moth *Plutella xylostella***

<http://researchonline.ljmu.ac.uk/id/eprint/11089/>

### Article

**Citation** (please note it is advisable to refer to the publisher's version if you intend to cite from this work)

**Wang, X, O'Reilly, AO, Williamson, MS, Puinean, AM, Yang, Y, Wu, S and Wu, Y (2018) Function and pharmacology of glutamate-gated chloride channel exon 9 splice variants from the diamondback moth *Plutella xylostella*. INSECT BIOCHEMISTRY AND MOLECULAR BIOLOGY. 104. pp.**

LJMU has developed **LJMU Research Online** for users to access the research output of the University more effectively. Copyright © and Moral Rights for the papers on this site are retained by the individual authors and/or other copyright owners. Users may download and/or print one copy of any article(s) in LJMU Research Online to facilitate their private study or for non-commercial research. You may not engage in further distribution of the material or use it for any profit-making activities or any commercial gain.

The version presented here may differ from the published version or from the version of the record. Please see the repository URL above for details on accessing the published version and note that access may require a subscription.

For more information please contact [researchonline@ljmu.ac.uk](mailto:researchonline@ljmu.ac.uk)

<http://researchonline.ljmu.ac.uk/>

Function and pharmacology of glutamate-gated chloride channel exon 9  
splice variants from the diamondback moth *Plutella xylostella*

Xingliang Wang <sup>a</sup>, Andrias O. O'Reilly <sup>b</sup>, Martin S. Williamson <sup>c</sup>, Alin. M. Puinean <sup>d</sup>, Yihua Yang <sup>a</sup>,  
Shuwen Wu <sup>a</sup>, Yidong Wu <sup>a,\*</sup>

<sup>a</sup> College of Plant Protection, Nanjing Agricultural University, Nanjing, China

<sup>b</sup> School of Natural Sciences and Psychology, Liverpool John Moores University, Liverpool, UK

<sup>c</sup> Biointeractions and Crop Protection Department, Rothamsted Research, Harpenden, UK

<sup>d</sup> Oxitec Limited, 71 Innovation Drive, Abingdon, Oxfordshire, UK.

*E-mail addresses:*

wxl@njau.edu.cn (X. Wang)

a.o.oreilly@ljmu.ac.uk (A. O. O'Reilly)

martin.williamson@rothamsted.ac.uk (M. S. Williamson)

mirel.puinean@oxitec.com (A. M. Puinean)

yhyang@njau.edu.cn (Y. Yang)

swwu@njau.edu.cn (S. Wu)

wyd@njau.edu.cn (Y. Wu)

1 **Abstract**

2 Glutamate-gated chloride channels (GluCl<sub>s</sub>) are found only in invertebrates and  
3 mediate fast inhibitory neurotransmission. The structural and functional diversity of  
4 GluCl<sub>s</sub> are produced through assembly of multiple subunits and via  
5 posttranscriptional alternations. Alternative splicing is the most common way to  
6 achieve this in insect GluCl<sub>s</sub> and splicing occurs primarily at exons 3 and 9. As  
7 expression pattern and pharmacological properties of exon 9 alternative splices in  
8 invertebrate GluCl<sub>s</sub> remain poorly understood, the cDNAs encoding three alternative  
9 splice variants (9a, 9b and 9c) of the PxGluCl gene from the diamondback moth  
10 *Plutella xylostella* were constructed and their pharmacological characterizations were  
11 examined using electrophysiological studies. Alternative splicing of exon 9 had little  
12 to no impact on PxGluCl sensitivity towards the agonist glutamate when subunits  
13 were singly or co-expressed in *Xenopus* oocytes. In contrast, the allosteric modulator  
14 abamectin and the chloride channel blocker fipronil had differing effects on PxGluCl  
15 splice variants. PxGluCl<sub>9c</sub> channels were more resistant to abamectin and PxGluCl<sub>9b</sub>  
16 channels were more sensitive to fipronil than other homomeric channels. In addition,  
17 heteromeric channels containing different splice variants showed similar sensitivity to  
18 abamectin (except for 9c) and reduced sensitivity to fipronil than homomeric channels.  
19 These findings suggest that functionally indistinguishable but pharmacologically  
20 distinct GluCl<sub>s</sub> could be formed in *P. xylostella* and that the upregulated constitutive  
21 expression of the specific variants may contribute to the evolution of insecticide  
22 resistance in *P. xylostella* and other arthropods.

23 **Key words**

24 Glutamate-gated chloride channel; alternative splicing; abamectin; fipronil;  
25 diamondback moth

## 1 **1. Introduction**

2 Chloride-conducting members of the cysteine loop ligand-gated ion channel (cys-loop LGIC)  
3 family play an important role in inhibitory synaptic transmission in the nervous systems of  
4 vertebrates and invertebrates.  $\gamma$ -aminobutyric acid (GABA)-gated chloride channels  
5 (GABACls) are extensively expressed in the nervous systems of arthropods and nematodes as  
6 well as in higher animals (Buckingham et al., 2005). In contrast, cys-loop glutamate-gated  
7 chloride channels (GluCls) are found only in invertebrates (Cull-Candy, 1976; Wolstenholme,  
8 2010). GABACls and GluCls are molecular targets for macrocyclic lactone insecticides  
9 (avermectins), which can activate these receptors directly, potentiate the response to the  
10 binding of their respective neurotransmitter or antagonize the agonist-induced channel current  
11 (Fuse et al., 2016; Wolstenholme, 2012). Phenylpyrazoles (e.g. fipronil) mainly target GABA  
12 receptors (Buckingham et al., 2005), but fipronil also showed inhibitory effects on GluCls,  
13 which acts as a blocker of these two types of LGICs (Kita et al., 2014; Narahashi et al., 2010;  
14 Wu et al., 2017; Zhao et al., 2004).

15 Cys-loop LGICs assemble as pentamers and each subunit has four transmembrane  
16 segments (TM1-TM4), a large N-terminal section that forms the extracellular  
17 neurotransmitter-binding domain and a comparatively smaller intracellular domain comprised  
18 mainly of the TM3-TM4 linker. LGICs can form as homomers or heteromers and different  
19 subunit combinations can produce receptors with diverse structural, functional and  
20 pharmacological properties. Six genes encode GluCl subunits in the nematode *Caenorhabditis*  
21 *elegans* and mite *Tetranychus urticae* (Jones & Sattelle, 2008; Dermauw et al., 2012). In  
22 contrast, GluCls in insect species are encoded by a single gene. Studies on several species of  
23 Diptera, Hymenoptera, Coleoptera, Hemiptera show that subunit diversity arises from  
24 posttranscriptional alternations of mRNA i.e. from splice variants and RNA editing (Furutani  
25 et al., 2014; Jones et al., 2010; Jones and Sattelle, 2006; Kita et al., 2014; Meyers et al., 2015;  
26 Semenov and Pak, 1999; Wang et al., 2016a; Wu et al., 2017). An invertebrate GluCl gene  
27 consists typically of 10 exons (Fig. 1A) and an overview of the five different processes that  
28 produce different subunit variants is shown in Fig 1B. In particular, exons 3 and 9 have been  
29 identified as "hot spot" domains of alternative splicing (Fig. 1B).

1 Exon 3 encodes a section of the extracellular ligand-binding domain and two variants in the  
2 5' region were first identified in *Drosophila melanogaster* (Semenov and Pak, 1999). These  
3 variants were initially termed modules 1 and 2 and correspond to exons 3a and 3b,  
4 respectively. To date, exon 3 alternative splice variants have been reported for the following  
5 insect species: *Apis mellifera* (Jones and Sattelle, 2006) and *Nasonia vitripennis* (Jones et al.,  
6 2010) have two alternatives whereas *Tribolium castaneum* (Jones and Sattelle, 2007), *Musca*  
7 *domestica* (Kita et al., 2014), *Bombyx mori* (Furutani et al., 2014), *Anopheles gambiae*  
8 (Meyers et al., 2015), *Plutella xylostella* (Wang et al., 2016a) and *Laodelphax striatellus* (Wu  
9 et al., 2017) have three alternatives. In addition, a fourth variant that lacks exon 3 was  
10 observed in *B. mori* (Furutani et al., 2014) and *P. xylostella* (our unpublished data).

11 Exon 9 encodes a section of the intracellular TM3-TM4 linker and, as with exon 3, variants  
12 in this region were also identified first in the *D. melanogaster* GluCl: a 12-bp stretch  
13 immediately downstream of an intron ending in AG results in four additional amino acids  
14 inserted before the predicted TM4 segment (Semenov and Pak, 1999). Similarly, a 21-bp  
15 stretch is found in the *L. striatellus* GluCl (Wu et al., 2017) and a 65-bp insertion is added  
16 downstream of the *P. xylostella* GluCl (PxGluCl) exon 9 (Liu et al., 2014). In addition, a  
17 33-bp insertion that was previously predicted to be part of intron 9 was found in *A. gambiae*  
18 GluCl (Meyers et al., 2015) (which the author defined as an additional exon 10 but we suggest  
19 is an exon 9 insertion following multi-sequences alignment analysis). In our previous study,  
20 alternative splicing of PxGluCl mRNA was detected in exon 9, which have three variants  
21 (exon 9a, 9b, 9c) as shown in Fig. 1 (Wang et al., 2016a). A 36-bp deletion variant (exon 9c in  
22 our study) was observed in an abamectin-resistant *P. xylostella* strain (Liu et al., 2014) and a  
23 partial deletion of exon 9 termed 9p $\Delta$  (also corresponding to exon 9c in our study) was found  
24 in *B. mori* GluCl (Furutani et al., 2014). Additionally, one exon skipping variant in the  
25 C-terminal amino acids sequences of *B. mori* GluCl was also detected in the larva brain  
26 (Furutani et al., 2014), which lacks the tenth exon.

27 Exon 3 splice variants have been well characterized in terms of GluCl function,  
28 pharmacology and spatiotemporal expression patterns (Furutani et al., 2014; Kita et al., 2014;  
29 Meyers et al., 2015; Wu et al., 2017). In contrast, little is known about the physiological roles

1 and pharmacology of GluCl<sub>s</sub> with exon 9 splice variants in the nervous system of any  
2 invertebrate. Therefore, in the present study we cloned and constructed the GluCl 9a, 9b and  
3 9c splice variants from the diamondback moth *P. xylostella*, a notorious pest of cruciferous  
4 vegetables worldwide. The three variants were expressed in *Xenopus* oocytes (both  
5 individually and in combination) and their electrophysiological responses examined with the  
6 endogenous agonist glutamate, the allosteric modulator abamectin (avermectin B1a) and the  
7 channel blocker fipronil. Our results demonstrate that functionally indistinguishable but  
8 pharmacologically distinct channels can form from alternative splice variants and we suggest  
9 the constitutive expression of these variants might affect insecticide toxicity in the field.

## 10 **2. Materials and methods**

### 11 *2.1. Chemicals*

12 L-Glutamic acid ( $\cong 99\%$ ) and fipronil (97.9%) were purchased from Sigma-Aldrich (St.  
13 Louis, MO, USA). Abamectin (B1a = 91.5%) was a gift from Veyong bio-chemical  
14 (Shijiazhuang, Hebei, CN). All the restricted enzymes used in this study, including *EcoRI*,  
15 *XbaI*, and *NotI* were purchased from Thermo Fisher Scientific (Waltham, MA, USA).

### 16 *2.2 Molecular cloning of PxGluCl splice variants*

17 Total RNA of 4<sup>th</sup>-instar larvae from the *P. xylostella* susceptible Roth strain was extracted  
18 by using the SV Total RNA Isolation System Kit (Promega, Madison, WI, USA) according to  
19 the manufacturer's protocol. First-strand cDNA was synthesized from 1  $\mu$ g total RNA using  
20 an oligo(dT)<sub>15</sub> primer and M-MLV reverse transcriptase (Promega). The cDNA of PxGluCl  
21 (isoform 9a) was cloned using PCR oligonucleotide primers PxGluCl\_ *EcoRI*\_F and  
22 PxGluCl\_ *XbaI*\_R (Table 1). This cDNA also provided the template for PxGluCl9b and  
23 PxGluCl9c PCR amplification using KAPA HiFi HotStart PCR Kit (KAPA Biosystems, USA)  
24 as follows. The upstream fragment of PxGluCl9b was amplified using primers  
25 PxGluCl\_ *EcoRI*\_F and PxGluC\_9b\_R, and the downstream fragment of PxGluCl9b was  
26 amplified using primers PxGluC\_9b\_F and PxGluCl\_ *XbaI*\_R (Table 1). Full-length  
27 PxGluCl9b was amplified by fusion PCR using the two fragments as the mixed template.  
28 Similarly, the full-length cDNA of PxGluCl9c was generated by the corresponding primers

1 (Table 1). The amplified full-length cDNA of each PxGluCl exon 9 splice variant was inserted  
2 into the cloning vector pJET1.2/blunt (Thermo Fisher Scientific, USA). After confirmation of  
3 their sequences (Eurofins Genomics, Germany), each recombinant plasmid of PxGluCl  
4 variant was digested with *EcoRI* and *XbaI* and the product (gel-purified) was ligated into the  
5 *EcoRI* and *XbaI* sites of the pGH19 vector, a modified version of plasmid pGEMHE, which  
6 contains 5'- and 3'-untranslated *X. laevis* beta-globin gene regions, and the presence of the  
7 variants were reconfirmed by nucleotide sequencing.

### 8 *2.3 cRNA synthesis and injection into Xenopus oocytes*

9 Each PxGluCl variant was extracted using the GeneJET plasmid miniprep kit (Thermo  
10 Scientific). Plasmids were linearized with *NotI*, and capped RNAs were generated using the  
11 T7 mMessage mMachine Kit (Ambion, Life Technologies, Paisley, UK) according to the  
12 manufacturer's instructions. Synthesized cRNAs were recovered by precipitation with  
13 isopropanol, dissolved in nuclease-free water at a final concentration of 500 ng/μL and stored  
14 at -80 °C until use.

15 Mature healthy *X. laevis* oocytes (stage V–VI) were treated with collagenase (type IA; 2  
16 mg/ml; Sigma, USA) in calcium-free Barth's solution (88 mM NaCl; 2.4 mM NaHCO<sub>3</sub>; 15  
17 mM Tris-HCl; 1 mM KCl; 0.82 mM MgCl<sub>2</sub>) for about 25 min at room temperature, rinsed  
18 three times, and manually defolliculated before injection with cRNA. Oocytes were injected  
19 with 32.2 nL cRNA (25 ng/μL) into the cytoplasm by using a Drummond variable volume  
20 microinjector. Alternatively, the oocytes were injected with a mixture of cRNAs (0.805 ng)  
21 composed of equal amount of two or three variants. After injection, calcium-containing  
22 Barth's solution (0.77 mM CaCl<sub>2</sub>) with antibiotics (100 units/mL penicillin, 100 μg/mL  
23 streptomycin, 4 μg/mL kanamycin and 50 μg/mL tetracycline) was used for oocyte incubation  
24 at 18 °C. Experiments were carried out 3-5 days after injection.

### 25 *2.4 Two-electrode voltage-clamp recordings*

26 *Xenopus* oocytes were held in a recording bath and continuously perfused with a Ringer's  
27 solution (115 mM NaCl, 2.5 mM KCl, 1.8 mM CaCl<sub>2</sub>, 10 mM HEPES, pH 7.3).  
28 Two-electrode voltage clamp was used for recording whole-cell currents from the injected

1 *Xenopus* oocytes. The glass capillary electrodes were filled with 3 M KCl and had a resistance  
2 of 0.5-1.5 M $\Omega$ . All the experiments were performed at 18-22 °C, and the induced inward  
3 currents were recorded with an OC-725C oocyte clamp (Warner Instruments, Hamden, CT,  
4 USA) at a holding potential of -60 mV. Data acquisition and analysis were carried out using  
5 iWorx 408 data acquisition system and LabScribe software (iWorx Systems, Inc. Dover, NH,  
6 USA). Glutamate was dissolved in Ringer's solution and applied to the oocytes for 3 s. After  
7 the glutamate perfusion, the oocytes were washed by Ringer's solution for 2 min to assess  
8 their reproducibility. Abamectin was first dissolved in DMSO (0.1 mM) and then diluted with  
9 Ringer's solution. The abamectin solution containing  $\leq 0.1\%$  DMSO was applied to oocytes  
10 for 15 s, and the oocytes were then washed for 3 min. For measuring response to abamectin,  
11 all oocytes were tested with one-shot application to avoid the carry-over effect from previous  
12 abamectin applications. The activated currents by abamectin applications were normalized to  
13 the saturating glutamate-induced current in the same oocyte. The chloride channel blocker  
14 fipronil was first dissolved in DMSO and then diluted with Ringer's solution ( $\leq 0.1\%$  DMSO).  
15 0.1 mM glutamate was first applied to oocytes 2-3 times to record a control response. After  
16 the last application of glutamate the oocytes were immediately perfused with fipronil for 2.5  
17 min, and then three further applications of 0.1 mM glutamate were made. For measuring  
18 inhibition by fipronil, all oocytes were tested with one-shot application protocol. The  
19 inhibition percentage was calculated from the average of two minimum responses to  
20 glutamate during the perfusion of fipronil. The same protocol was used for all variant  
21 channels. Fifty percent effective concentrations (EC<sub>50</sub>s), Hill coefficients (nHs), and 50%  
22 inhibitory concentrations (IC<sub>50</sub>s) were obtained from dose-response curves that were analyzed  
23 by nonlinear regression analysis using GraphPad Prism 5.0 (GraphPad Software Inc., San  
24 Diego, CA, USA). Data were obtained from at least four oocytes from at least two frogs.

## 25 *2.5 Statistics*

26 Data are given as means  $\pm$  SEM. Statistical analysis was determined by a one-way  
27 ANOVA multiple comparison test or Student's *t*-test. Significance was set up at alpha = 0.05.

## 28 **3. Results**



### 1 3.1 Molecular cloning of PxGluCl splice variants

2 The full-length cDNA of PxGluCl3c9a was amplified from the susceptible Roth *P.*  
3 *xylostella* strain then subcloned and sequenced in our previous work (Wang et al., 2016a).  
4 This transcript (GenBank accession no. JX014231.1, referred to as '9a' in this study) consists  
5 of 1347-bp nucleotides that encode a protein of 448 amino acids. Two naturally occurring  
6 splice variants: PxGluCl9b and PxGluCl9c (referred to as 9b and 9c in this study, respectively)  
7 were also reported in Wang et al., 2016a. In the present study a high-fidelity fusion PCR  
8 strategy, using the 9a cDNA as template, the 9b and 9c splice variants were successfully  
9 amplified and confirmed by nucleotide sequencing (GenBank accession nos. MH459002 and  
10 MH459003). The translated protein sequences show that 9b and 9c have a loss of 9 and 12  
11 amino acids, respectively, at the alternative 3' acceptor site of exon 9, which encodes a part of  
12 the TM3-TM4 intracellular loop (Fig. 1C). To generate expression plasmids for  
13 electrophysiological studies, each of the three PxGluCl splice variants was subcloned into the  
14 pGH19 vector and verified by nucleotide sequencing.

### 15 3.2 Sensitivity of PxGluCl splice variants to glutamate

16 The alternatively spliced PxGluCl constructs 9a, 9b and 9c were expressed individually in  
17 *X. laevis* oocytes and the glutamate responses of these homomeric channels were recorded by  
18 two-electrode voltage-clamp technique. Glutamate concentration-response curves (C-R curves)  
19 were measured by applying concentrations ranging from 0.3  $\mu$ M to 1 mM for each construct  
20 (see the sample traces shown in Fig. 2A). The application of glutamate to the three channels  
21 induced robust concentration-dependent inward currents, demonstrating that functional  
22 homomers can be formed by all splice variants. Meanwhile, application of glutamate in the  
23 same concentration range to control oocytes showed no response (data not shown). The C-R  
24 curves for 9a, 9b and 9c channels gave  $EC_{50}$ s of  $17.70 \pm 3.73 \mu$ M,  $19.04 \pm 1.99 \mu$ M and  $21.89$   
25  $\pm 3.24 \mu$ M, respectively (Table 2, Fig. 2B). No significant differences were observed in the  
26  $EC_{50}$ s and nHs among the three splice variants expressed singly in oocytes ( $p > 0.05$ ).

27 As it is possible that heteromeric PxGluCls may assemble *in vivo* in *P. xylostella*, we  
28 measured the glutamate responses from oocytes co-injected with two or three different

1 cRNAs. Glutamate C-R curve was generated from concentrations ranging from 0.1  $\mu$ M to 0.1  
2 mM for each construct. The C-R curves gave  $EC_{50}$ s of  $8.21 \pm 0.95 \mu$ M for 9a+9b,  $9.54 \pm 1.67$   
3  $\mu$ M for 9a+9c,  $15.83 \pm 1.19 \mu$ M for 9b+9c and  $13.57 \pm 1.20 \mu$ M for 9a+9b+9c channels  
4 (Table 2, Fig. 2C). When compared with co-expressed 9b+9c channels, the potencies of  
5 glutamate in 9a+9b and 9a+9c heteromeric expressions were increased by 1.9- and 1.7-fold,  
6 respectively, significant differences in  $EC_{50}$ s were observed ( $p < 0.05$ ), and reduction in nHs  
7 of 9a+9b was also significant (Dunnett's Multiple Comparison Test,  $p < 0.05$ ). Meanwhile, the  
8 Hill coefficient of 9b+9c and 9a+9b+9c were  $2.2 \pm 0.39$  ( $n = 9$ ),  $2.20 \pm 0.31$  ( $n = 8$ ),  
9 respectively, suggesting that more than one glutamate molecule is required to activate these  
10 two co-expressed channels.

### 11 3.3 Sensitivity of PxGluCl splice variants to abamectin

12 The allosteric activator abamectin induced robust, slowly activating and irreversible  
13 currents (see the sample traces in Fig. 3A) for all channels in a concentration-dependent  
14 fashion (Fig. 3). As shown in the Table 2, the  $EC_{50}$ s of abamectin calculated from C-R curves  
15 of singly expressed 9a, 9b and 9c channels were  $0.13 \pm 0.04 \mu$ M,  $0.28 \pm 0.12 \mu$ M and  $1.07 \pm$   
16  $0.78 \mu$ M, respectively (Fig. 3B). When compared with 9a channels, 9b appeared less sensitive  
17 to abamectin with a 2.2-fold increase in  $EC_{50}$  but this difference was not significant ( $p > 0.05$ ).  
18 In contrast, singly injected 9c oocytes showed significant reduction in sensitivity to abamectin.  
19 The  $EC_{50}$  of 9c was increased by 8.2-fold, and the nH of 9c was reduced by 3.7-fold. Both of  
20 the changes in  $EC_{50}$  and nH were significantly (Dunnett's Multiple Comparison Test,  $p < 0.05$ ),  
21 which suggests that the absence of 12 amino acids in the TM3-TM4 loop of 9c channels  
22 results in abamectin insensitivity at the receptor level.

23 We also examined abamectin responses on the PxGluCl variants co-expressed in oocytes.  
24 The C-R curves gave  $EC_{50}$ s of  $0.18 \pm 0.09 \mu$ M for 9a+9b,  $0.20 \pm 0.11 \mu$ M for 9a+9c,  $0.23 \pm$   
25  $0.15 \mu$ M for 9b+9c and  $0.32 \pm 0.26 \mu$ M for 9a+9b+9c channels (Table 2, Fig. 3C). Abamectin  
26 activated each co-expressed channel with a similar  $EC_{50}$  and the change range among the four  
27  $EC_{50}$ s was no more than 1.8-fold. No significant change in the  $EC_{50}$ s and nHs among oocytes  
28 co-injected with different PxGluCl variant cRNAs were observed ( $p > 0.05$ ), suggesting  
29 oocytes co-expressed two or three variants showed a similar response to abamectin.

### 3.4 Sensitivity of PxGluCl splice variants to fipronil

Fipronil, a ligand-gated chloride channels blocker with insecticidal potency, was used to test whether alternative splicing produces differences in the pharmacological properties of PxGluCls. The perfusion of fipronil reduced glutamate-induced inwards currents (see the sample traces in Fig. 4A). The C-R curves of fipronil for 9a, 9b and 9c channels gave IC<sub>50</sub>s of 10.22 ± 4.08 μM, 3.79 ± 2.02 μM, and 12.92 ± 7.65 μM, respectively (Table 2, Fig. 4B). The 9b channels were more sensitive to this compound than 9a channels (unpaired t test, t=1.764 df=8, p = 0.1158) and 9c channels (unpaired t test with Welch's correction, t=1.924 df=4, p = 0.1266), with 2.7- and 3.4-fold reduction in IC<sub>50</sub>s.

The IC<sub>50</sub>s of fipronil for PxGluCls composed of different variants were 55.45 ± 19.48 μM for 9a+9b, 32.67 ± 21.09 μM for 9a+9c, 16.47 ± 6.92 μM for 9b+9c and 57.99 ± 14.55 μM for 9a+9b+9c (Table 2, Fig. 4C). Inhibition by fipronil was not significantly different among the four co-expressed channels (p > 0.05). Interestingly, the potencies of fipronil to the heteromeric expressed PxGluCls were lower than that of the homomeric-expressed PxGluCls to some extent (Table 2).

## 4. Discussion

Field populations of the *P. xylostella* pest have evolved various levels of resistance to 95 active ingredients (APRD, 2018), including abamectin (Pu et al., 2010) and fipronil (Wang et al., 2016b) pesticides that act on GluCls. We previously identified three mutually exclusive splice variants of *P. xylostella* GluCl exon 3 (Wang et al., 2016a) and in this current study we focused on exon 9 splice variants. We show that 9a, 9b and 9c variants expressed individually or co-expressed in oocytes produce robust inward currents in a dose-dependent pattern in response to glutamate. In addition, abamectin or fipronil either induced or inhibited inward currents, respectively, and there was a significant difference in GluCl sensitivity to these compounds depending on the expressed exon 9 variant.

Resistance to avermectins has been associated with point mutations of GluCls in *C. elegans*, *D. melanogaster*, *T. urticae* and *P. xylostella* (Dent et al., 2000; Dermauw et al., 2012; Kane et al., 2000; Kwon et al., 2010; Wang et al., 2016a; Wang et al., 2017). Our

1 electrophysiological study found a 8.2-fold reduction in abamectin sensitivity with the exon  
2 9c 12-aa deletion isoform when compared to 9a, which is the most common type of PxGluCl  
3 (described in Wang et al., 2016a and Wang et al., 2017). In addition, the exon 9b 9-aa deletion  
4 of PxGluCl also reduced the sensitivity to abamectin by 2.2-fold compared with 9a. Another  
5 study of *P. xylostella* (Liu et al., 2014) found that the expression of exon 9c produced a shift  
6 in the EC<sub>50</sub> of abamectin from 118 nM to 1146 nM, which was about 10-fold higher than that  
7 of wild type channels. In contrast, with *B. mori* a partial deletion of exon 9 named 9pΔ  
8 (corresponding to the exon 9c of PxGluCl) had almost no impact on ivermectin action  
9 (Furutani et al., 2014).

10 The inhibitory potencies of fipronil differed among the three variants, with 9b showing  
11 more sensitivity (2.7- to 3.4-fold) than 9a or 9c isoforms. Furthermore, all heteromeric  
12 channels showed lower sensitivity to fipronil than homomeric channels. We found that  
13 fipronil inhibited glutamate-induced currents in PxGluCls with micromolar IC<sub>50</sub>s (Table 2).  
14 These IC<sub>50</sub>s values are significantly higher than found with other insects and nematodes,  
15 where IC<sub>50</sub>s range from 10 nM to 2930 nM with the exception of *C. elegans* glc-3 (IC<sub>50</sub> of  
16 11.5 μM). These findings suggest that substantial variations in sensitivity to fipronil can occur  
17 between different species. Although PxGluCls are considered the secondary target of fipronil  
18 after GABA<sub>A</sub> receptors, it is possible that the upregulated constitutive expression of 9a, 9c or  
19 heteromeric channels may enhance synergistic resistance to fipronil in the field.

20 The individual 9a, 9b and 9c splice variants appear to have a similar sensitivity towards  
21 glutamate as we found no significant difference in the EC<sub>50</sub>s and nHs between homomeric  
22 channels. Similarly in *L. striatellus* there were no significant differences in the response of  
23 LsGluCl-AL (a 21-bp stretch observed immediately downstream of intron 8) channel to  
24 glutamate, when compared with the LsGluCl-AS (the normal sequence) channel (Wu et al.,  
25 2017). However, other studies did find differences in glutamate sensitivity depending on the  
26 exon 9 transcript. With the *B. mori* GluCl the 9pΔ deletion (corresponding to PxGluCl exon  
27 9c) had a small effect on glutamate action (Furutani et al., 2014). An even greater difference  
28 was found in an earlier study of *P. xylostella* GluCl where exon 9c variant was found to be  
29 about 13-fold less sensitive to glutamate compared to the wild-type (exon 9a) receptor (Liu et

1 al., 2014).

2 The intracellular domain remains the most poorly characterized region of LGIC receptors.  
3 Only the structures of acetylcholine and serotonin receptors have part of their TM3-TM4  
4 linkers resolved (Unwin, 2005; Basak et al., 2018). These structures have an alpha-helical  
5 region of about 20 residues termed the ‘MA’ helix that precedes TM4 and extends into the  
6 cytoplasm where MAs meet to form a pentameric helix bundle. Although this structural  
7 feature may be conserved in GluCl receptors, the region encoded by the exon 9 variants is  
8 further than 20 residues from TM4 and is therefore predicted to lie just beyond the putative  
9 MA helix. We speculate that variation in this region may affect inter-monomer packing by the  
10 MA helices. As each MA helix is contiguous with TM4, a change in MA packing could be  
11 propagated via contact with TM4 to effect the conformation of the transmembrane domain  
12 and reposition residues that are ligand-binding determinants. Therefore an allosteric  
13 modification of the avermectin and fipronil binding sites may explain the effect of splice  
14 variants on GluCl sensitivity towards these two compounds. The structural effects exerted by  
15 the splice variants may not be propagated as far as the extracellular domain, which could  
16 account for the similar glutamate sensitivity of all the GluCls investigated in our study.  
17 However, a previous study with PxGluCl exon 9a and 9c variants did find a significant  
18 difference in glutamate sensitivity (Liu et al., 2014), which suggests the involvement of  
19 another mechanism. It is possible that post-translational modifications mediated by the  
20 TM3-TM4 linker can effect GluCl glutamate sensitivity. We note that the TM3-TM4 linkers  
21 of nAChR and 5-HT3A receptors provide sites for post-translational modifications, which  
22 may affect channel trafficking, kinetics and desensitization (McKinnon et al., 2012; Tsetlin et  
23 al., 2011).

24 In summary, we functionally characterized and determined pharmacological properties of  
25 a complete set of alternative PxGluCl exon 9 splices and our results provide evidence that an  
26 as yet uncharacterized region of LGICs can have an impact on receptor pharmacology. We  
27 found that the shortest variant 9c is associated with a decreased sensitive to abamectin  
28 whereas homomers formed from the medium-length 9b variant are more sensitive to fipronil.  
29 The physiological roles of the different homomeric and heteromeric assembled channels

1 remain to be examined but our study indicates that monitoring the frequency of the splice  
2 variants may provide a valuable molecular approach to evaluating the development of  
3 abamectin and fipronil resistance in the field.

#### 4 **Acknowledgements**

5 This work was supported by grants from National Natural Science Foundation of China  
6 (31772196 and 31301693), the Chinese Ministry of Agricultural 948 project (2014-S10).  
7 Rothamsted Research also receives grant-aided support from the UK Biotechnology and  
8 Biological Sciences Research Council (BBSRC).

#### 9 **References**

- 10 APRD, 2018. Arthropod Pesticide Resistance Database. <http://www.pesticideresistance.org/>.  
11 (accessed in 5 Mar. 2018).
- 12 Basak, S., Gicheru, Y., Samanta, A., Molugu, S.K., Huang, W., Fuente, M. la de, Hughes, T.,  
13 Taylor, D.J., Nieman, M.T., Moiseenkova-Bell, V., Chakrapani, S., 2018. Cryo-EM  
14 structure of 5-HT<sub>3A</sub> receptor in its resting conformation. *Nat. Commun.* 9, 514.
- 15 Buckingham, S.D., Biggin, P.C., Sattelle, B.M., Brown, L.A., Sattelle, D.B., 2005. Insect  
16 GABA receptors: splicing, editing, and targeting by antiparasitics and insecticides. *Mol.*  
17 *Pharmacol.* 68, 942-951.
- 18 Cull-Candy, S.G., 1976. Two types of extrajunctional L-glutamate receptors in locust muscle  
19 fibres. *J. Physiol.* 255, 449-464.
- 20 Dent, J.A., Smith, M.M., Vassilatis, D.K., Avery, L., 2000. The genetics of ivermectin  
21 resistance in *Caenorhabditis elegans*. *Proc. Natl. Acad. Sci. U S A* 97, 2674-2679.
- 22 Dermauw, W., Ilias, A., Riga, M., Tsagkarakou, A., Grbic, M., Tirry, L., Van Leeuwen, T.,  
23 Vontas, J., 2012. The cys-loop ligand-gated ion channel gene family of *Tetranychus*  
24 *urticae*: implications for acaricide toxicology and a novel mutation associated with  
25 abamectin resistance. *Insect Biochem. Mol. Biol.* 42, 455-465.
- 26 Furutani, S., Ihara, M., Nishino, Y., Akaike, A., Jones, A.K., Sattelle, D.B., Matsuda, K., 2014.  
27 Exon 3 splicing and mutagenesis identify residues influencing cell surface density of  
28 heterologously expressed silkworm (*Bombyx mori*) glutamate-gated chloride channels.  
29 *Mol. Pharmacol.* 86, 686-695.
- 30 Fuse, T., Kita, T., Nakata, Y., Ozoe, F., Ozoe, Y., 2016. Electrophysiological characterization  
31 of ivermectin triple actions on *Musca* chloride channels gated by L-glutamic acid and  
32 gamma-aminobutyric acid. *Insect Biochem. Mol. Biol.* 77, 78-86.
- 33 Jones, A.K., Bera, A.N., Lees, K., Sattelle, D.B., 2010. The cys-loop ligand-gated ion channel  
34 gene superfamily of the parasitoid wasp, *Nasonia vitripennis*. *Heredity* 104, 247-259.
- 35 Jones, A.K., Sattelle, D.B., 2006. The cys-loop ligand-gated ion channel superfamily of the  
36 honeybee, *Apis mellifera*. *Invert. Neurosci.* 6, 123-132.
- 37 Jones, A.K., Sattelle, D.B., 2007. The cys-loop ligand-gated ion channel gene superfamily of  
38 the red flour beetle, *Tribolium castaneum*. *BMC Genomics* 8,327.

- 1 Jones, A.K., Sattelle, D.B., 2008. The cys-loop ligand-gated ion channel gene superfamily of  
2 the nematode, *Caenorhabditis elegans*. *Invert. Neurosci.* 8, 41-47.
- 3 Kane, N.S., Hirschberg, B., Qian, S., Hunt, D., Thomas, B., Brochu, R., Ludmerer, S.W.,  
4 Zheng, Y., Smith, M., Arena, J.P., Cohen, C.J., Schmatz, D., Warmke, J., Cully, D.F.,  
5 2000. Drug-resistant *Drosophila* indicate glutamate-gated chloride channels are targets  
6 for the antiparasitics nodulisporic acid and ivermectin. *Proc. Natl. Acad. Sci. U S A* 97,  
7 13949-13954.
- 8 Kita, T., Ozoe, F., Ozoe, Y., 2014. Expression pattern and function of alternative splice  
9 variants of glutamate-gated chloride channel in the housefly *Musca domestica*. *Insect*  
10 *Biochem. Mol. Biol.* 45, 1-10.
- 11 Kwon, D.H., Yoon, K.S., Clark, J.M., Lee, S.H., 2010. A point mutation in a glutamate-gated  
12 chloride channel confers abamectin resistance in the two-spotted spider mite,  
13 *Tetranychus urticae* Koch. *Insect Mol. Biol.* 19, 583-591.
- 14 Liu, F., Shi, X.Z., Liang, Y.P., Wu, Q.J., Xu, B.Y., Xie, W., Wang, S.L., Zhang, Y.J., Liu, N.N.,  
15 2014. A 36-bp deletion in the alpha subunit of glutamate-gated chloride channel  
16 contributes to abamectin resistance in *Plutella xylostella*. *Entomol. Exp. Appl.* 153,  
17 85-92.
- 18 McKinnon, N.K., Bali, M., Akabas, M.H., 2012. Length and amino acid sequence of peptides  
19 substituted for the 5-HT3A receptor M3-M4 loop may affect channel expression and  
20 desensitization. *PLoS One* 7, e35563.
- 21 Meyers, J.I., Gray, M., Kuklinski, W., Johnson, L.B., Snow, C.D., Black, W.C., Partin, K.M.,  
22 Foy, B.D., 2015. Characterization of the target of ivermectin, the glutamate-gated  
23 chloride channel, from *Anopheles gambiae*. *J. Exp. Biol.* 218, 1478-1486.
- 24 Narahashi, T., Zhao, X., Ikeda, T., Salgado, V.L., Yeh, J.Z., 2010. Glutamate-activated  
25 chloride channels: unique fipronil targets present in insects but not in mammals. *Pestic.*  
26 *Biochem. Physiol.* 97, 149-152.
- 27 Unwin, N., 2005. Refined structure of the nicotinic acetylcholine receptor at 4A resolution. *J.*  
28 *Mol. Biol.* 346, 967-989.
- 29 Pu, X., Yang, Y.H., Wu, S.W., Wu, Y.D., 2010. Characterisation of abamectin resistance in a  
30 field-evolved multiresistant population of *Plutella xylostella*. *Pest Manag. Sci.* 66,  
31 371-378.
- 32 Semenov, E.P., Pak, W.L., 1999. Diversification of *Drosophila* chloride channel gene by  
33 multiple posttranscriptional mRNA modifications. *J. Neurochem.* 72, 66-72.
- 34 Tsetlin, V., Kuzmin, D., Kasheverov, I., 2011. Assembly of nicotinic and other Cys-loop  
35 receptors. *J. Neurochem.* 116, 734-741.
- 36 Wang, X., Wang, R., Yang, Y., Wu, S., O'Reilly, A.O., Wu, Y., 2016a. A point mutation in the  
37 glutamate-gated chloride channel of *Plutella xylostella* is associated with resistance to  
38 abamectin. *Insect Mol. Biol.* 25, 116-125.
- 39 Wang, X.L., Wu, S.W., Gao, W.Y., Wu, Y.D., 2016b. Dominant inheritance of field-evolved  
40 resistance to fipronil in *Plutella xylostella* (Lepidoptera: Plutellidae). *J. Econ. Entomol.*  
41 109, 334-338.
- 42 Wang, X.L., Puinean, A.M., O'Reilly, A.O., Williamson, M.S., Smelt, C.L.C., Millar, N.S.,  
43 Wu, Y.D., 2017. Mutations on M3 helix of *Plutella xylostella* glutamate-gated chloride  
44 channel confer unequal resistance to abamectin by two different mechanisms. *Insect*

1 Biochem. Mol. Biol. 86, 50-57.  
2 Wolstenholme, A.J., 2010. Recent progress in understanding the interaction between  
3 avermectins and ligand-gated ion channels: putting the pests to sleep. *Invert. Neurosci.*  
4 10, 5-10.  
5 Wolstenholme, A.J., 2012. Glutamate-gated chloride channels. *J. Biol. Chem.* 287,  
6 40232-40238.  
7 Wu, S.F., Mu, X.C., Dong, Y.X., Wang, L.X., Wei, Q., Gao, C.F., 2017. Expression pattern  
8 and pharmacological characterisation of two novel alternative splice variants of the  
9 glutamate-gated chloride channel in the small brown planthopper *Laodelphax striatellus*.  
10 *Pest Manag. Sci.* 73, 590-597.  
11 Zhao, X.L., Yeh, J.Z., Salgado, V.L., Narahashi, T., 2004. Fipronil is a potent open channel  
12 blocker of glutamate-activated chloride channels in cockroach neurons. *J. Pharmacol.*  
13 *Exp. Ther.* 310, 192-201.  
14



15 Table 1. Sequences of primers used in this study.

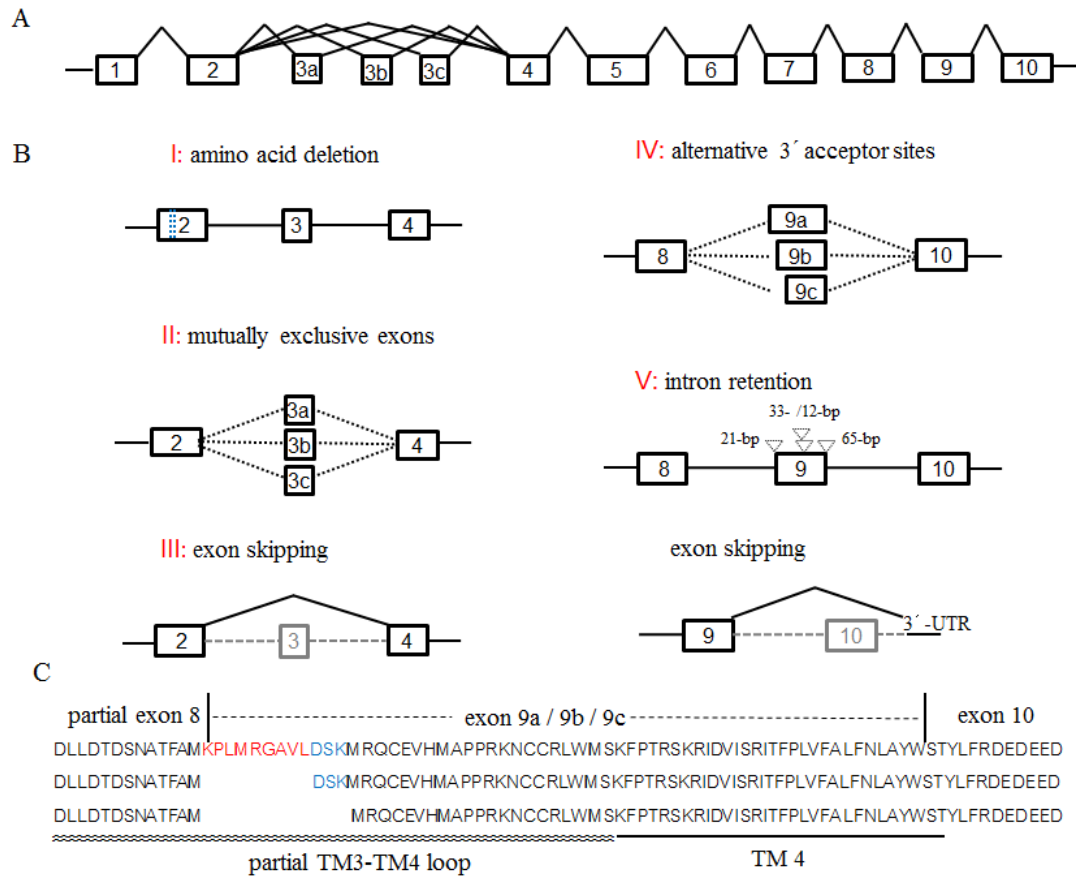
Primer	Purpose	Sequence (5' to 3')
PxGluCl_EcoRI_F	Full-length cDNA amplification and fusion PCR	CGGAATTCGGTTTGCTGAGTTGGAGAATGGACG
PxGluCl_XbaI_R	Full-length cDNA amplification and fusion PCR	GCTCTAGATGCCAGTGGAACGATGCTGATGC
PxGluC_9b_F	Amplify the downstream fragment of 9b variant	CTTCGCGATGGACTCCAAGATGCGACAGTG
PxGluC_9b_R	Amplify the upstream fragment of 9b variant	TCTTGGAGTCCATCGCGAAGGTGGCATTG
PxGluC_9c_F	Amplify the downstream fragment of 9c variant	TTCGCGATGATGCGACAGTGCGAGGTG
PxGluC_9c_R	Amplify the upstream fragment of 9c variant	CACTGTCGCATCATCGCGAAGGTGGCATTG

16 Table 2. Effects of glutamate and abamectin on membrane currents, and the effects of fipronil on glutamate-induced membrane currents from *Xenopus* oocytes  
 17 containing variant subunits singly or co-expressed *PxGluCls*, with EC<sub>50</sub> and IC<sub>50</sub> values shown. Data are the mean ± SEM from n = 4 - 9 oocytes from 2 to 3 different  
 18 frogs.

Variants	L-glutamate			Abamectin			Fipronil		
	n	EC <sub>50</sub> μM	n <sub>H</sub>	n	EC <sub>50</sub> μM	n <sub>H</sub>	n	IC <sub>50</sub> μM	n <sub>H</sub>
Singly expressed									
Exon 9a	7	17.70 ± 3.73	1.21 ± 0.37	7	0.13 ± 0.04	1.29 ± 0.08	5	10.22 ± 4.08	0.56 ± 0.09
Exon 9b	6	19.04 ± 1.99	1.60 ± 0.19	5	0.28 ± 0.12	0.60 ± 1.16	5	3.787 ± 2.02	0.48 ± 0.03
Exon 9c	6	21.89 ± 3.24	1.60 ± 0.22	5	1.07 ± 0.78 <sup>†</sup>	0.35 ± 0.02	6	12.92 ± 7.65	0.43 ± 0.07
Co-expressed									
Exon 9a+9b	6	8.21 ± 0.95 <sup>*</sup>	1.12 ± 0.21	5	0.18 ± 0.09	0.99 ± 0.07	5	55.45 ± 19.48	0.50 ± 0.12
Exon 9a+9c	6	9.54 ± 1.67 <sup>*</sup>	1.33 ± 0.10	5	0.20 ± 0.11	1.03 ± 0.09	4	32.67 ± 21.09	0.45 ± 0.03
Exon 9b+9c	9	15.83 ± 1.19	2.20 ± 0.39	4	0.23 ± 0.15	1.07 ± 0.15	5	16.47 ± 6.92	0.31 ± 0.04
Exon 9a+9b+9c	8	13.57 ± 1.20	2.20 ± 0.31	5	0.32 ± 0.26	0.58 ± 0.11	4	57.99 ± 14.55	0.49 ± 0.09

31 \* Indicates that the glutamate EC<sub>50</sub>s for 9a+9b and 9a+9c are significantly different to 9b+9c, but not to 9a+9b+9c (alpha = 0.05).

32 † Indicates the abamectin EC<sub>50</sub>s for 9c is significantly different to 9a, but not to 9b (alpha = 0.05).



33

34 **Figure 1.** Genomic structure and alternative splicing of the glutamate-gated chloride channel. (A)

35 Typical genomic organization of GluCl. Exons are shown as boxes and introns as thin angled

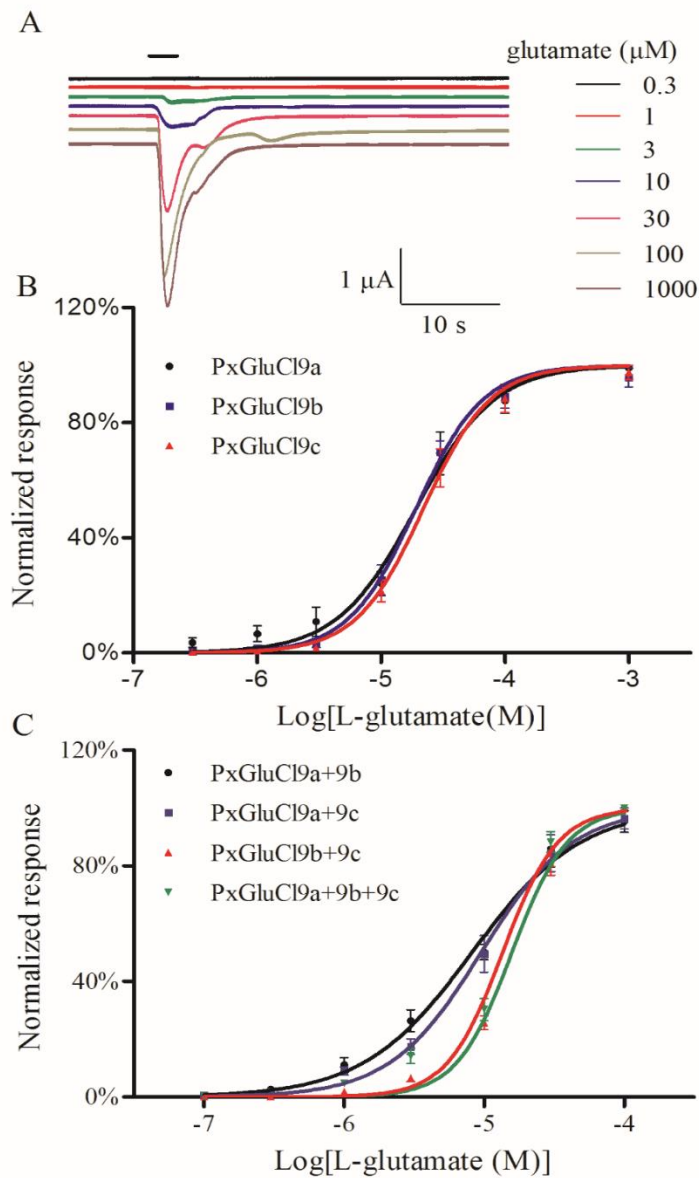
36 lines. (B) Reported alternative splice variants and amino acids deletion of GluCl. The deletion of

37 four amino acids in exon 2 is indicated by blue dotted line and the insertions of partial introns are

38 indicated by inverted triangles. (C) Sequence alignment of three PxGluCl splice variants: 9a (top),

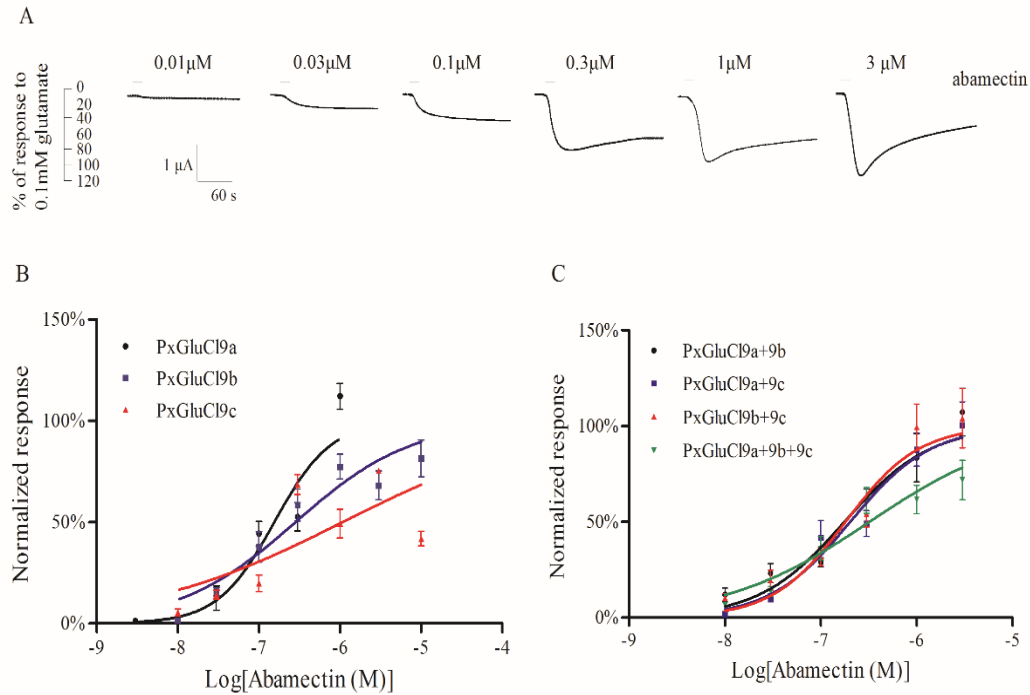
39 9b (middle) and 9c (bottom). The partial TM3-TM4 loop and TM4 domains are indicated by wavy

40 lines and a horizontal thick line, respectively.

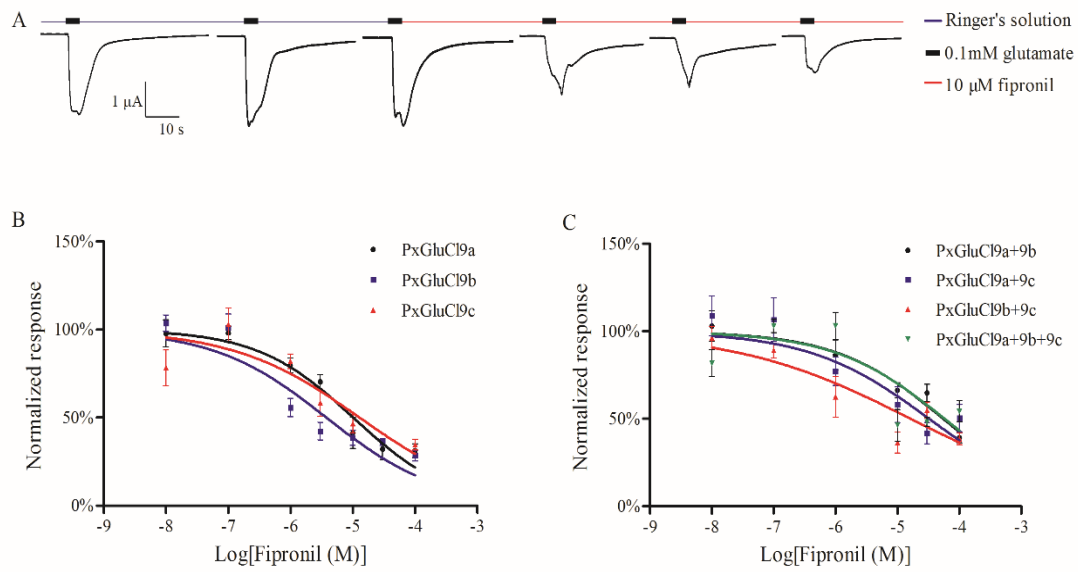


41

42 **Figure 2.** Glutamate responses of *PxGluCl*s containing variant subunits singly or co-expressed in  
 43 *Xenopus* oocytes. (A) Representative current traces induced by glutamate from 0.3  $\mu\text{M}$  to 1 mM in  
 44 channels containing singly expressed 9a variant. (B) Glutamate concentration response curves  
 45 from singly expressed variants. (C) Glutamate concentration response curves from co-expressed  
 46 variants. Data are the mean  $\pm$  SEM from  $n = 6 - 9$  oocytes from 2 to 3 different frogs.



47  
 48 **Figure 3.** Abamectin responses of *PxGluCl*s containing variant subunits singly or co-expressed in  
 49 *Xenopus* oocytes. (A) Representative current traces induced by abamectin from 0.01 μM to 3 μM  
 50 in channels containing singly expressed 9a variant. (B) Abamectin concentration response curves  
 51 obtained for singly expressed variants. (C) Abamectin concentration response curves obtained for  
 52 co-expressed variants. Data are the mean ± SEM from n = 4 - 7 oocytes from 2 to 3 different frogs.



53

54 **Figure 4.** Fipronil inhibition of glutamate-induced responses of *PxGluCls* containing variant  
 55 subunits singly or co-expressed in *Xenopus* oocytes. (A) Representative current traces showing the  
 56 effect of 10 μM fipronil on the 0.1 mM glutamate response in channels containing singly  
 57 expressed 9a variant. (B) Fipronil concentration response curves obtained for singly expressed  
 58 variants. (C) Fipronil concentration response curves obtained for co-expressed variants. Data are  
 59 the mean ± SEM from n = 4 - 6 oocytes from 2 to 3 different frogs.